

The extent of error-prone replication-restart by homologous recombination is controlled by Exo1 and checkpoint proteins

Article (Published Version)

Carr, Antony, Lambert, Sarah A E, Tsang, Ellen, Miyabe, Izumi, Iraqui, Ismail and Zheng, Jiping (2014) The extent of error-prone replication-restart by homologous recombination is controlled by Exo1 and checkpoint proteins. *Journal of Cell Science*, 127 (13). pp. 2983-2994. ISSN 0021-9533

This version is available from Sussex Research Online: <http://sro.sussex.ac.uk/49409/>

This document is made available in accordance with publisher policies and may differ from the published version or from the version of record. If you wish to cite this item you are advised to consult the publisher's version. Please see the URL above for details on accessing the published version.

Copyright and reuse:

Sussex Research Online is a digital repository of the research output of the University.

Copyright and all moral rights to the version of the paper presented here belong to the individual author(s) and/or other copyright owners. To the extent reasonable and practicable, the material made available in SRO has been checked for eligibility before being made available.

Copies of full text items generally can be reproduced, displayed or performed and given to third parties in any format or medium for personal research or study, educational, or not-for-profit purposes without prior permission or charge, provided that the authors, title and full bibliographic details are credited, a hyperlink and/or URL is given for the original metadata page and the content is not changed in any way.

The extent of error-prone replication-restart by homologous recombination is controlled by Exo1 and checkpoint proteins.

Ellen Tsang^{1#}, Izumi Miyabe^{1#}, Ismail Iraqi^{3#}, Jiping Zheng², Sarah A. E. Lambert^{3*}, and Antony M. Carr^{1*}.

¹ Genome Damage and Stability Centre, University of Sussex, Brighton, Sussex, BN1 9RQ, UK.

² Dept of Biotechnology, College of Agriculture, No.58 Renmin Avenue, Haikou, Hainan Province, 570228 P.R. China.

³ Institut Curie-Centre National de la Recherche Scientifique, UMR3348, Réponse cellulaire aux perturbations de la réplication, centre universitaire, Bat 110, 91405 Orsay, France.

Word count: 7897

Figures: 5

Supl Figures: 3

Running title: Regulation of collapsed-fork processing

* Corresponding authors: S. Lambert (Sarah.Lambert@curie.fr); A.M. Carr (a.m.carr@sussex.ac.uk)

These authors contributed equally

Key words: checkpoint, genome instability, homologous recombination

Abstract

Genetic instability, a hallmark of cancer, can occur when the replication machinery encounters a barrier. The intra-S phase checkpoint maintains stalled replication forks in a replication-competent configuration by phosphorylating replisome components and DNA repair proteins to prevent forks from catastrophically collapsing. Here we report a novel Chk1- and Cds1^{Chk2}-independent function for Rad3^{ATR}, the core *S. pombe* checkpoint sensor kinase: Rad3^{ATR} regulates the association of recombination factors with collapsed forks thus limiting their genetic instability. We further reveal antagonistic roles for Rad3^{ATR} and the 9-1-1 clamp: Rad3^{ATR} restrains MRN- and Exo1-dependent resection while the 9-1-1 complex promotes Exo1 activity. Interestingly the MRN complex, but not its nuclease activity, promotes resection and the subsequent association of recombination factors at collapsed forks. The biological significance of this regulation is revealed by the observation that Rad3^{ATR} prevents Exo1-dependent genome instability upstream a collapsed fork without affecting the efficiency of recombination-mediated replication-restart. We propose the interplay between Rad3^{ATR} and the 9-1-1 clamp functions to fine-tune the balance between the need for recovery of replication via recombination and the risk of increased genome instability.

Introduction

Replicative stress can be caused by a wide variety of situations including: tightly bound protein-DNA complexes; clashes of the replication machinery with other cellular processes (i.e. transcription); the presence of non-canonical DNA structures; and nucleotide precursor depletion (Lambert and Carr, 2013a). The intra-S phase checkpoint acts within S phase and promotes cell survival and genome stability in response to replicative stress (Lindsay et al., 1998; Lopes et al., 2001; Tercero and Diffley, 2001) by stabilising arrested forks. In all organisms studied, the intra-S phase checkpoint requires the activity of two kinases: a phosphoinositol-3 kinase-like kinase (PIKK), known in metazoans as ATR, that senses replication problems by interacting directly with single stranded DNA (ssDNA) binding proteins (Zou and Elledge, 2003) and a downstream checkpoint kinase that is directly activated by ATR via interactions with the mediator protein, Claspin (Errico and Costanzo, 2012; Segurado and Tercero, 2009).

In the fission yeast *Schizosaccharomyces pombe*, the ATR homolog is known as Rad3^{ATR} and the downstream effector kinase for the intra-S phase checkpoint is Cds1^{Chk2} (Lindsay et al., 1998). As is the case in mammalian cells, but not for the budding yeast *Saccharomyces cerevisiae*, the heterotrimeric checkpoint clamp complex, composed of Rad9, Rad1 and Hus1 (9-1-1) is also essential for the intra S-phase checkpoint (Errico and Costanzo, 2012). Activation of the intra-S phase checkpoint results in phosphorylation of a wide range of replication proteins and DNA repair proteins (Bailis et al., 2008; Boddy et al., 2000; Chen et al., 2010; De Piccoli et al., 2012; Hu et al., 2012; Miyabe et al., 2009; Segurado and Tercero, 2009; Smolka et al., 2007). The precise details as to how these phosphorylation events regulate DNA replication and DNA metabolism to stabilise the arrested fork remains largely obscure. In part, this is because we do not yet have the full range of phosphorylation events mapped and phenotypically characterised. It is also because, in the absence of the intra-S phase checkpoint, the DNA structures that are initially present at the replication fork in S phase are processed (Sogo et al., 2002) into different structures (i.e. into ssDNA and double strand breaks; DSBs (Sabatinos et al., 2012)). These can both signal through the G2 DNA damage checkpoint and be repaired in a distinct manner from the original lesion. Further complicating genetic analysis, the DNA damage checkpoint requires the function of many of

the same proteins as the intra-S phase checkpoint, with the exceptions that the effector kinase and mediator proteins are replaced (Carr, 2002; Stracker et al., 2009).

Experimentally, replication stress is often imposed by treating cells with the ribonucleotide reductase inhibitor, hydroxyurea (HU) to globally inhibit replication. During the subsequent dNTP depletion, the intra-S phase checkpoint stabilises the slowed-down replication forks in a replication-competent state (Lopes et al., 2001). Here we will refer to these as a “stalled” fork. Stalled forks can resume replication without intervention by additional mechanisms when the blockade is removed. In contrast, HU treatment in the absence of the intra-S phase checkpoint results in replication forks that cannot resume (Sabatinos et al., 2012; Sogo et al., 2002). We refer to these as “collapsed” forks. Fork collapse likely occurs when the activities of the replicative helicase and the replicative polymerases are uncoupled, generating extensive stretches of ssDNA. Collapsed forks can also result from clashes between replisomes and the transcription machinery, or with tightly DNA-bound protein complexes. It has been reported that collapsed forks are no longer associated with components of the replisome, i.e. the replication machinery is not available for DNA synthesis (Cobb et al., 2003; Cobb et al., 2005; Katou et al., 2003; Lucca et al., 2004). However, this may be a simplification and the machinery may still be present, but no longer able to resume replication (De Piccoli et al., 2012).

Irrespective of the precise nature of the replication machinery present at collapsed forks, it has been demonstrated that, in the absence of the intra-S phase checkpoint, the genome of HU treated yeast cells is degraded by nucleases including Mus81 (Boddy et al., 2000; Froget et al., 2008; Kai et al., 2005) and Exo1 (Cotta-Ramusino et al., 2005; Lopes et al., 2001; Segurado and Diffley, 2008; Sogo et al., 2002) and that this degradation is prevented, at least in part, by the phosphorylation of a range of replication proteins and proteins that process specific DNA structures (Chen et al., 2010; De Piccoli et al., 2012; Hu et al., 2012; Segurado and Tercero, 2009; Smolka et al., 2007). The precise physical consequences of fork collapse at the level of the resulting DNA structure remains largely unclear. It is also not clear if the phenomenon of fork collapse is a cause or consequence of inappropriate DNA processing. However, once a fork does collapse, the DNA is exposed to recombination events that can potentially lead to genome instability (Alabert et al., 2009; Barlow and Rothstein, 2009; Iraqui et al., 2012; Lambert et al., 2010; Lambert et al., 2005; Lisby et al., 2004; Meister et

al., 2005; Mizuno et al., 2009; Myung et al., 2001; Myung and Kolodner, 2002; Segurado and Diffley, 2008).

Nucleotide depletion is only one of many potential barriers to replication. While avoiding fork collapse is one key function of the intra-S phase checkpoint, in certain situations the collapse of an arrested replication fork may be preferable to its stabilisation. In other cases, replication fork collapse may be unavoidable: for example, when the replisome is blocked by an inter-strand crosslink there is not likely to be sufficient ssDNA to activate the Intra-S phase checkpoint. Interestingly, loss of the intra-S phase effector kinase Cds1^{Chk2} in fission yeast increases viability of otherwise wild-type cells to treatment with the DNA inter-strand crosslinking agent nitrogen mustard (Lambert et al., 2003). This suggests that the initial activation of the checkpoint effector kinase is detrimental to cell survival in these circumstances (reviewed in (Lambert and Carr, 2013a)). There is indirect evidence to suggest that the intra-S phase checkpoint proteins regulate the use of recombination for the subsequent repair or restart of collapsed replication forks (Haghnazari and Heyer, 2004; Pandita et al., 2006; Sorensen et al., 2005). However, the mechanisms by which the checkpoint proteins might facilitate recombination at collapsed replication forks are not clear: for example, checkpoint proteins may function to directly promote recombination or they may favour certain recombination pathways over others (Haghnazari and Heyer, 2004; Kolodner et al., 2002).

The activation of the intra-S phase checkpoint and its components have been largely characterised in response to acute replication stress (such as HU treatment) whereas the cellular response to chronic and endogenous replication stress is less well characterised, despite the fact this represents the main source of replication-induced genetic instability in pre-neoplastic lesions (Bester et al., 2011; Halazonetis et al., 2008). In this report we have therefore used an established replication fork barrier (RFB) that induces a local and chronic replication stress to explore the ATR-dependent checkpoint response. The RFB we have exploited is the *RTS1* sequence in fission yeast. *RTS1* is a well characterised polar RFB that requires a sequence specific Myb-domain DNA binding protein, Rtf1, for its function (Lambert and Carr, 2005; Lambert et al., 2010).. In wild-type *S. pombe* cells, *RTS1* resides close to the mating type (*mat*) locus and, when bound by Rtf1, functions to block replication forks passing in one direction while allowing them to pass unhindered in the opposite

direction (Eydmann et al., 2008). While *RTSI*:Rtf1 is not directly involved in mating-type switching, its barrier activity facilitates switching by preventing inappropriate forks moving through the switching region in the wrong direction (Codlin and Dalgaard, 2003; Dalgaard and Klar, 2001; Lee et al., 2004). In our experimental systems, either one or two copies of the 850 bp *RTSI* sequence are positioned at the *ura4* locus (Figures 1A and 2B) and *rtf1*⁺, which is essential for *RTSI* RFB activity, is under control of a thiamine-repressible *nmt* promoter. Upon induction of *rtf1*⁺ transcription, forks arrest and rapidly collapse (Lambert et al., 2005). Recombination proteins are required for fork restart (Lambert et al., 2010), which occurs within 20 minutes (unpublished data). There is no cell cycle arrest resulting from this DNA processing (Figure S1) (Lambert et al., 2005), consistent with there being sufficient time within the normal cell cycle to restart the collapsed forks by homologous recombination (HR).

Results

Checkpoint genes are not essential in the RuraR system

Using a construct where two *RTSI* sequences are integrated at the *ura4* locus as inverted repeats flanking *ura4*⁺ (*RuraR*) we have previously demonstrated that, when forks arrest at *RTSI*, they are subject to recombination-mediated restart (Lambert et al., 2005). Greater than 94% of forks arrest when they encounter the RFB and the vast majority restart correctly (Lambert et al., 2010; Mizuno et al., 2013) within 20 minutes and complete replication. In the *RuraR* system (Figure 1A), cell viability is impaired when the recombination pathway, but not the *rad3*^{ATR} checkpoint protein, is compromised (Lambert et al., 2005) and no cell cycle delay is observed when the *RTSI*-RFB was induced ((Lambert et al., 2005) and Suppl. Figure S1). To extend this observation we crossed the *RuraR* locus into *cds1* and *chk1* (downstream effector kinases), *rad17* (checkpoint clamp loader) and *rad9* (9-1-1 checkpoint clamp subunit) null backgrounds. We used a micro-colony assay to establish the percentage of cells able to form colonies of greater than 10 cells when replication arrest was either induced or not induced. We confirmed that (unlike recombination-defective *RuraR* control strains) viability was not significantly affected by checkpoint loss: *rad3*, *rad9*, *rad17*, *cds1* and *chk1* null *RuraR* cells were all able to form micro-colonies as efficiently as the

checkpoint-proficient *RuraR* strain (Figure 1B). In order to rule out the possibility that checkpoint mutants are defective for *RTS1*-dependent RFB activity we assayed replication intermediates in *rad3* null and *rad3*⁺ control strains grown both with and without thiamine. The extent of fork pausing at *RuraR* in *rad3* null cells (98.4 % ±1.2 of arrested forks) was comparable to that observed for wild-type (97.3 % ±1.8) (Figure 1C).

Thus, replication completion upon activation of the *RTS1*-RFB does not require checkpoint pathways or cell-cycle delay. This is in contrast to acute replication stresses caused by agents such as hydroxyurea. These circumstances thus allow us to separate the known roles of the intra-S phase and replication checkpoints - promoting replication resumption by preventing fork collapse and delaying the cell cycle, respectively - away from any potential functions in either regulating DNA metabolism at a collapsed fork or in regulating the ensuing choice of HR pathway. We thus set out to examine the recruitment of HR proteins to the collapsed fork at *RTS1* and to observe potential changes to aberrant recombination outcomes caused by loss of checkpoint proteins.

Regulation of Rad52 recruitment by checkpoint proteins

We previously demonstrated that induction of replication fork arrest at *RTS1* leads to the recruitment of Rad52 to the *RuraR* locus (Lambert et al., 2005). To establish if the extent of recruitment is subject to checkpoint regulation, we performed Chromatin immunoprecipitation (ChIP) analyses against Rad52-GFP in checkpoint-mutated *RuraR* strains (Figure 1D) following growth for 40 hours either with thiamine (arrest “off”) or without thiamine (arrest “on”). Transcription is induced by the *nmt41* promoter approximately 16 hours following thiamine removal (Maundrell, 1993). Thus, at 40 hours in the absence of thiamine, the culture is in a steady state where forks arrest at *RuraR* during each S phase and replication of the locus is reliant on HR-dependent fork restart. Consistent with this, we have previously demonstrated that fork arrest at *RuraR* is not detectable 12 hours following thiamine removal but occurs with similar efficiency at both 24 or 48 hours after thiamine removal ((Lambert and Carr, 2005); c.f. Figure 1).

In the wild-type strain background, “arrest on” conditions resulted in Rad52 recruitment at, and immediately flanking, the *RuraR* locus (Figure 1D, top panel, blue bars). As expected, enrichment was most prevalent at the right hand (centromere (*cen*)-proximal) barrier, since

Journal of Cell Science • Accepted manuscript

the direction of replication fork movement is from right to left (Mizuno et al., 2013). Enrichment persisted for approximately 2kb *cen*-proximal to the *RTS1* sequence. A second less prevalent region of enrichment extended approximately 1 kb from the left hand barrier towards the telomere (*tel*). In the *rad3*^{ATR} null background, Rad52 recruitment was significantly increased, both at *RTS1* sequences and in the flanking regions, and spread further behind the fork arrest site, >3 Kb *cen*-proximal to the *RTS1* sequence (Figure 1D, top panel, red bars). To better visualise the role of Rad3^{ATR} in regulating Rad52-association at the *RuraR* locus, Rad52-enrichment in *rad3-d* cells was calculated relative to that observed for the wild-type control (Figure 1D, bottom panel). This confirmed that Rad52 was up to six times enriched at both *tel* and *cen*-proximal regions flanking the *RTS1*-RFB in *rad3-d* cells when compared to *rad3*⁺.

In contrast to the higher recruitment of Rad52 in the *rad3* null strain, in both the *rad17* (clamp loader, Figure 1E) and *rad9* (9-1-1 complex subunit, Suppl. Figure 2A,B) null strains Rad52 recruitment was significantly reduced by approximately two fold at *RTS1* sequences and at both the *tel*- and *cen*-proximal flanking sequences relative to wild-type. We also assessed the effect of the double *rad3*^{ATR} *rad17* null mutant. This showed a Rad52 recruitment profile similar to that of *rad17* null cells (Figure 1E), indicating that the effect of losing Rad3^{ATR} function requires a functional Rad17/9-1-1 clamp. Interestingly, neither the *chk1* nor the *cds1*^{Chk2} null strains showed a reproducible change in the Rad52 recruitment when compared to wild-type (Suppl. Figure 2C), a result consistent with there being no evidence for checkpoint-dependent cell cycle arrest (Suppl. Figure 1). These data show that the checkpoint sensor Rad3^{ATR} prevents the extensive recruitment of Rad52 upstream of arrested forks, whereas the sensor Rad17-dependent 9-1-1 clamp loading promotes such Rad52 recruitment. Moreover, the function of checkpoint sensors in regulating Rad52 association at collapsed forks is independent of the downstream effector kinases Chk1 and Cds1^{Chk2}. To address whether the regulation of Rad52 association by the checkpoint proteins is related to the formation of single stranded DNA at blocked forks we next investigated the role of nuclease activities in Rad52 association.

Regulation of Rad52 recruitment by MRN and Exo1

In response to a DNA double strand break (DSB), the MRN complex functions to initiate resection (Mimitou and Symington, 2008; Raynard et al., 2008; Symington, 2002).

Subsequent ssDNA generation is largely Exo1-dependent, with a later contribution from Rqh1^{RecQ} and Dna2. When a fork collapses at *RTS1* there is no DSB formation (Mizuno et al., 2009) and HR-dependent replication restart occurs from a single-stranded gap (Lambert et al., 2010). To establish if MRN or the Exo1 nuclease participate in DNA metabolism at *RTS1*-induced collapsed forks we investigated the involvement of MRN and Exo1 in Rad52 loading. When the replication fork arrest was induced in a *rad50* null strain, Rad52 recruitment to *RuraR* was reduced relative to wild-type (Figure 2A, left panels). Similarly, the increased recruitment of Rad52 in the *rad3* null background was also reduced. In contrast to *rad50* null cells, the *rad32^{mre11}-D65N* nuclease-deficient allele (Hartsuiker et al., 2009) had no effect on Rad52 enrichment levels in either the *rad3⁺* or *rad3* null strains (Figure 2A). Thus, an intact MRN complex, but not the nuclease activity of Rad32^{Mre11}, is required for Rad52 recruitment and the increased loading observed in a *rad3* null background is similarly MRN-dependent.

Exo1 has been implicated with Mre11 in the resection of DSBs to generate ssDNA (Mimitou and Symington, 2008; Moreau et al., 1999; Moreau et al., 2001; Tsubouchi and Ogawa, 2000; Zhu et al., 2008). Exo1 has been reported to be negatively regulated by Mec1^{ATR} and Rad53^{Chk2} in the generation of ssDNA at uncapped telomeres in budding yeast (Jia et al., 2004; Morin et al., 2008; Zubko et al., 2004). Again in *S. cerevisiae*, during DNA replication Exo1 is proposed to travel with active replication forks and participates in the instability of stalled forks in the absence of regulation by Rad53^{Chk2} (Cotta-Ramusino et al., 2005; Segurado and Diffley, 2008). In our analysis, an *exo1* null strain shows a significant decrease of Rad52 recruitment at *RuraR*, both in the *rad3⁺* background and in combination with a *rad3* null mutant (Figure 2A, right panel). Thus, at collapsed forks, Exo1 is required for normal Rad52 recruitment at single stranded gaps in checkpoint proficient cells and mediates the extensive Rad52 loading observed in *rad3* null cells.

RPA, Rad52 and Rad51 are recruited upstream the site of fork arrest

Rad52 is known to bind to RPA-coated ssDNA, replacing the RPA to initiate homologous recombination by nucleating Rad51 filaments (Krejci et al., 2012). Thus, Rad52 recruitment immediately upstream of the site of fork collapse is strongly indicative of DNA processing. We next verified that both Rpa1 and Rad51 were also recruited with similar profiles. To clearly distinguish the recruitment of proteins either upstream or downstream the collapsed

fork, we used the *uraR* construct in which a single *RTS1* barrier is located *cen*-proximal to *ura4⁺* (Lambert et al., 2010) (Figure 2B). The use of the *uraR* locus simplifies the analysis since the *RuraR* locus, in addition to recombination-mediated fork restart at the site of fork collapse, is also subjected to recombination events dependent on a template switch between the two inverted *RTS1* repeats (Lambert et al., 2010). Such events could influence the location of Rad52 recruitment in the vicinity of the *RTS1*-RFB (Lambert et al., 2010).

Similar to the increased Rad52 association observed at *RuraR*, the binding of Rad52, Rad51 and RPA were all increased at *uraR* in *rad3* null cells when compared to *rad3⁺* controls, particularly upstream of the site of fork arrest (Figure 2C). The association of these single stranded binding proteins to *uraR* were also dependent on Rad17 and Exo1, as observed for the *RuraR* construct. Moreover, the double *rad17 exo1* null mutant showed a similar reduction in Rad52 binding upstream the *RTS1*-RFB as each single mutant, suggesting that Rad17 and Exo1 act in a same pathway of Rad52 recruitment at arrested forks (Figure 2C). These data are consistent with Rad3^{ATR} limiting extensive Exo1-dependent resection behind collapsed forks, and the PCNA-like 9-1-1 complex promoting it.

Checkpoint proteins do not influence template exchange at RuraR

Taken together, our data strongly imply that DNA is resected upstream a collapsed replication fork in a manner dependent on Rad17 and the 9-1-1 complex, MRN and Exo1 and is attenuated by the activity of Rad3^{ATR}. We have previously reported that the majority of arrested forks rapidly restart correctly by HR and complete replication, but that in the *RuraR* system, 2-5% of cells/generation undergo inappropriate template exchange with the nearby inverted repeat (Lambert et al., 2010; Lambert et al., 2005; Mizuno et al., 2009). This results in intra-chromosomal recombination, leading to either inversion of the *ura4* gene or the formation of an acentric and dicentric chromosome (Suppl. Figure 3). Both these events can be monitored by Southern blot and pulse field gel analysis and, upon fork arrest, the frequency of the rearrangement-specific band increases with each generation. We thus analysed wild-type, checkpoint-null and *exo1*-null *RuraR* cultures at T₀ (fork arrest “off”) and after 48 hours growth without thiamine, T₄₈ (fork arrest “on”), for fork arrest-induced recombination intermediates (2-dimensional gel electrophoresis (2DGE); Suppl. Figure 3B,C) and for both recombination outcomes: acentric chromosome formation (Suppl. Figure 3D) and *ura4⁺* inversion (Suppl. Figure 3E).

In *rad3*, *rad17* and *exo1* null mutant backgrounds, recombination intermediates (D loops and structures containing Holliday junctions) were visualised at levels equivalent to the wild type control and the recombination outcomes were unchanged. Thus, the perturbation in resection and in recombination protein loading seen in the checkpoint mutants or the *exo1* mutant did not significantly influence the amount of HR-dependent replication restart after fork collapse or the types of deleterious intra-chromosomal recombination events that occur due to faulty template exchange between *RTS1* sequences at *RuraR*. Our data therefore suggest that a limited amount of recombination factors are sufficient to promote replication restart by template exchange.

Extensive resection behind the fork results in increased genetic instability

Our data are consistent with a model whereby the extent of resection upstream of the collapsed fork is not rate-limiting for fork restart. However, extensive resection such as that seen in the *rad3* null mutant background implies that restart must frequently occur a significant distance upstream of the point of the original fork collapse. To establish if this is the case, we visualised the converging fork signal (Figure 3A) by 2DGE analysis. In a wild type background ~8% of the replication intermediates represent converging forks that we assume arise when an incoming replisome from the *tel*-proximal side approaches the arrested fork structure close to, or within, *RTS1*. In *rad17* or *exo1* null backgrounds this signal remained constant. However, in *rad3* null cells, where resection is proposed to be extensive, the signal is reduced >3 fold (Figure 3B,C). This is consistent with the expectation that resection beyond the restriction site *cen*-proximal to *RTS1* (that defines the fragment being analysed by 2DGE, see the right cartoon on 3A) would result in a restart event upstream of the initial point of fork collapse and thus loss of the converging fork signal within the restriction fragment analysed by 2DGE. Concomitant loss of *exo1* in the *rad3* null mutant restored the converging fork signal to the wild type level, consistent with loss of the termination signal being a consequence of extensive resection

The restart of the collapsed fork upstream of the initial site of arrest would result in more DNA being replicated by the restarted replication machine. We have previously shown that restarted replication forks are prone to replication slippage at microhomology (Iraqi et al., 2012). Using an assay where replication slippage removes a short direct repeat from the *ura4-sd20* allele, we therefore tested for evidence that the region upstream the blocked fork

Journal of Cell Science • Accepted manuscript

is more susceptible to such slippage errors when resection is extensive (Figure 4). First, the spontaneous level of replication slippage (irrespective of whether Rtf1 was overexpressed or not) was similar in all the genetic backgrounds tested (*RTS1*-RFB is absent: see construct 1 on Figure 4). Second, fork-arrest led to an equivalent increase in replication slippage downstream the *RTS1*-RFB during replication restart in all genetic backgrounds (see construct 2 on figure 4A). This observation confirms that, whatever the level of recombination factors associated with the collapsed replication fork, replication-restart occurred efficiently. Third, when the marker gene was placed upstream of the *RTS1*-RFB, fork-arrest in checkpoint proficient cells led to three fold increase in replication slippage that is occurring upstream of the site of fork arrest ($p < 1.7 \cdot 10^{-5}$) (see construct 3 on figure 4). This is consistent with occasional leading strand degradation and subsequent re-synthesis by an HR-restarted replication fork upstream of the initial site of fork arrest (Iraqi et al., 2012). The induction in replication slippage upstream of the site of replication arrest is Exo1-dependent ($p < 0.0002$). A 1.9 fold induction in replication slippage was observed in *rad17* null mutant cells, although this was not statistically significant ($p > 0.05$). In contrast, fork-arrest led to a 8.7 fold increase in replication slippage upstream of the arrest site in the *rad3* null mutant ($p < 9.8 \cdot 10^{-5}$), corresponding to a 2.9 times higher level when compared to the *rad3*⁺ strain ($p < 1.6 \cdot 10^{-5}$). Replication slippage occurring upstream the *RTS1*-RFB in *rad3* null cells was dependent on both Exo1 and Rad17 ($p < 8.2 \cdot 10^{-6}$). These data strongly support our model that the efficiency of HR-dependent restart does not require checkpoint activation, but frequently occurs upstream of the site of initial arrest when resection is extensive.

It can also be predicted that the generation of ssDNA behind the collapsed fork would increase opportunities for homologous recombination to occur erroneously upstream the site of the initial fork arrest. To establish if the increased DNA processing behind the fork increased non-allelic homologous recombination in this region, we turned to a direct repeat recombination assay (Ahn et al., 2005). It is proposed that recombination between the direct repeats requires nuclease activities to resect nascent strands until a homologous region is exposed as ssDNA (Sun et al., 2008). In this system, two *ade6* heteroalleles are positioned as direct repeats that flank a *his3*⁺ marker and a single *RTS1* barrier (Figure 5A). Replication is predicted to run from right to left at this locus (Heichinger et al., 2006) and, consistent with

this, Ahn et al (2005) (Ahn et al., 2005) demonstrated that the *RTS1* barrier orientation must arrest right-to-left forks to significantly elevate recombination rates.

Ahn et al (2005) (Ahn et al., 2005) assayed recombination in the presence of constitutive *rtf1* expression. In order to regulate fork arrest, we combined a thiamine-repressible *nmt41-rtf1* allele with their *ade6*-heteroallele locus and scored *ade6* recombination in the wild-type, *rad3* and *exo1* null backgrounds at T₀ (no induced arrest) and after 48 hours either with (arrest “off”) or without (arrest “on”) thiamine (Figure 5B). It should be noted that the “arrest off” conditions (+ thiamine) retain a low, but significant, levels of fork arrest (Lambert et al., 2010; Lambert et al., 2005) and thus do not fully reflect recombination in the complete absence of arrest. Nonetheless, *rad3* null mutants in “arrest on” conditions showed elevated levels of recombination ($p < 0.0019$) when compared to *rad3*⁺ cells (18.9 v 11.79 recombinants per 10³ cells) and *exo1* null cells show significantly reduced levels ($p < 0.0004$) of recombination (5.06 v 11.79 recombinants per 10³ cells). Importantly, concomitant deletion of *exo1* in the *rad3* null background reduced the level of recombination in the “arrest on” conditions to levels approaching those of the *exo1* null single mutant (6.88 vs 5.06 recombinants per 10³ cells). These data suggest that *RTS1*-induced *ade6* heteroallele recombination is suppressed by Rad3^{ATR}, promoted by Exo1 activity and that Rad3^{ATR} is inhibiting Exo1-dependent recombination.

Discussion

The role of the intra-S phase checkpoint in maintaining arrested replication forks in a replication competent state is well documented and the mechanisms underlying how this is achieved are beginning to be unravelled. In this report we identify a new function for the intra-S phase checkpoint at collapsed replication forks. Specifically, we show that the recruitment of RPA, Rad52 and Rad51 to the site of a collapsed fork is distinctively controlled by Rad3^{ATR} and the 9-1-1 checkpoint clamp through the co-ordination of Exo1 and MRN-dependent resection (Figure 5C). This checkpoint regulation of DNA processing limits the extent of local replication errors that occur as a consequence of HR-dependent replication restart. Moreover, our work reveals a role for the checkpoint sensors, independently of the downstream kinases, in limiting replication-induced genome instability in response to a chronic replication stress, thus contrasting with the classical analysis of checkpoint activation in response to acute replication stress.

The role of checkpoint proteins at RTS1-blocked replication forks

An active replisome moves with the fork and closely couples DNA synthesis to the activity of the replicative helicase (Errico and Costanzo, 2012). The current model is that, if polymerisation is perturbed, the helicase initially moves ahead of the polymerases to expose an additional ~100bp of ssDNA (Sogo et al., 2002). This promotes the stimulation of Rad3^{ATR} and local activation of the intra-S phase checkpoint. The checkpoint kinases (in *S. pombe*; Rad3^{ATR} and Cds1^{Chk2}) subsequently phosphorylate a range of replication and repair proteins. This protects the fork from collapse and retains the replisome in an active conformation (De Piccoli et al., 2012) while at the same time arresting cell cycle progression. Conversely, if helicase activity is perturbed, as opposed to polymerisation, the initial exposure of ssDNA does not occur, the intra-S phase checkpoint is not activated, the replisome cannot be held in an active conformation and the fork will collapse (Lambert and Carr, 2013a).

By analogy with the *E. coli* Tus-ter site-specific replication fork barrier (Bastia et al., 2008) and the Reb1-dependent barrier at the *S. pombe* rDNA locus (Biswas and Bastia, 2008), we speculate that forks arrest at *RTS1* because the replicative helicase is directly inhibited by the *RTS1*-associated proteins. Thus, because the helicase cannot move ahead of the polymerases,

ssDNA is not formed, Rad3^{ATR} is not activated and the fork collapses. By analysing the association of single-stranded DNA binding proteins with a specific collapsed replication fork we have been able to show that the Rad3^{ATR} checkpoint is locally activated by fork collapse to ultimately control the activity of subsequent DNA processing events. Because forks arrested at *RTS1* do not require the intra S-phase checkpoint for their restart, we have been able to use our model systems to specifically examine the processing of DNA at the site of fork collapse, independently of the consequences of replisome stabilisation. Our data show that Rad3^{ATR}-dependent regulation of Exo1-dependent resection results in inappropriate DNA processing of the collapsed fork, but that this does not prevent HR-dependent replication restart.

Previous work has identified Exo1 as a significant target of the intra-S phase checkpoint when ATR is activated to stabilise intact replisomes: in *S. cerevisiae*, Rad53^{Chk2} prevents Exo1-dependent replication fork breakdown in response to global replication stress (Cotta-Ramusino et al., 2005; Segurado and Diffley, 2008) and Rad53^{Chk2} has also been suggested to phosphorylate and regulate Exo1 at uncapped telomeres (Morin et al., 2008). In mammalian cells, Exo1 has been shown to be phosphorylated at 12 sites, of which 3 are induced by HU treatment in an ATR-dependent manner (Bolderson et al., 2010; El-Shemerly et al., 2008). Thus, our identification of Exo1 as a key target of the ATR pathway at collapsed forks as well as when forks are being stabilised emphasises the importance of regulating this nuclease.

Mechanistically, we show that the PCNA-like 9-1-1 checkpoint clamp acts to promote MRN- and Exo1-dependent resection of DNA to extend a region of ssDNA upstream the collapsed replication fork. This function for the clamp loader/clamp axis of the checkpoint is regulated by Rad3^{ATR}, but not by Chk1 or Cds1^{Chk2}. Thus, in the absence of Rad3^{ATR} function and the presence of a loaded 9-1-1 complex, repair-protein recruitment is likely increased. Unfortunately, we have been unable to generate reagents that can ChIP Exo1. However, the likely explanation is that Rad3^{ATR} directly phosphorylates the clamp loader/clamp subunits and/or specific repair proteins recruited by the clamp (candidates include Mre11 and Exo1) to restrict resection. Such a mode of regulation would be fully consistent with the multiple phosphorylation events reported for these proteins.

Checkpoint regulation of recombination-protein recruitment contributes to genome stability

Replication stress underlies a significant proportion of the genomic instability observed in model organisms and in cancer cells (Carr and Lambert, 2013; Lambert and Carr, 2013b; Segurado and Tercero, 2009). The intra-S phase checkpoint is essential for maintaining the integrity of replication forks in the presence of such stress (Errico and Costanzo, 2012). Loss of the ability to maintain the replication-competent state of arrested/paused replication forks leads to their collapse, an event that has been linked to increased genome rearrangements in *S. cerevisiae* (Cha and Kleckner, 2002; Kaochar et al., 2010; Myung et al., 2001; Myung and Kolodner, 2002) and the expression of fragile sites in humans (Brown and Baltimore, 2003; Casper et al., 2002; Durkin et al., 2006). We have previously reported that, when a fork collapses, replication restart occurs via a ssDNA intermediate, not from a DSB (Mizuno et al., 2009). We found that fork restart is highly efficient, but prone to non-allelic homologous recombination (NAHR), i.e. it has an approximately 1-3% chance of restarting at a the wrong place if a homologous sequence is nearby (Lambert and Carr, 2005; Lambert et al., 2010). We also demonstrated that, once restarted correctly, the restarted replication machinery is prone to replication slippage at microhomology (Iraqi et al., 2012) or to performing a U-turn at closely-spaced inverted repeats (Mizuno et al., 2013).

As a consequence of fork collapse and restart, NAHR (associated with the restart event) and replication slippage (associated with the restarted replisome) provide mechanisms for the genomic instability associated replication stress. We examined the effects of the Rad3^{ATR} checkpoint on these genome instability mechanisms that are specifically related to collapsed forks, as opposed to stalled forks and their subsequent resumption of replication. Somewhat to our surprise, we found that recombination-mediated fork restart was independent of the checkpoint and the frequency of the associated NAHR was unchanged. These data suggest that even limited association of recombination factors at collapsed replication forks is sufficient to ensure their efficient restart. However, the extensive resection we observed in the *rad3* null mutant prompted us to explore if this additional DNA processing resulted in more extensive genetic instability associated with the error prone nature of the restarted replication fork and intra/inter sister chromatid homologous recombination.

We observed that the extent of resection and subsequent recombination protein recruitment correlated directly to the promotion (*rad3 null*) or suppression (*rad17 null*) of inter/intra

sister HR. These data implicate Rad3^{ATR} in limiting genome instability by regulating DNA metabolism and thus the activity of HR behind collapsed replication forks. We also observed a correlation between replication slippage after restart and the extent of resection. These data are entirely consistent with increased resection resulting in a larger region of DNA being replicated by an error prone restarted fork. Thus, a function of Rad3^{ATR} is to limit the amount of DNA replicated by the restarted fork, which in turn reduces the likelihood of associated genetic instability.

Conclusions

It has become clear that the inter-S phase checkpoint, acting through Rad3^{ATR} and Cds1^{Chk2} in *S. pombe*, Mec1^{ATR} and Rad53^{Chk2} in *S. cerevisiae* or ATR and Chk1 in human cells, prevents replication forks catastrophically collapsing, in part by phosphorylating replisome components and specific proteins affecting DNA metabolism such as Exo1 (Reviewed in (Errico and Costanzo, 2012; Segurado and Tercero, 2009)). A recent report also showed that moderate replication stress in ATR depleted mammalian cells results in MRN-dependent ssDNA accumulation, the chromatin association of checkpoint sensors and common fragile site (CFS) expression (Koundrioukoff et al., 2013). Here, using a site-specific replication arrest system, we have dissected the role of Rad3^{ATR} in fork stabilisation and checkpoint activation away from those occurring after the fork has collapsed. We reveal a subtle role for the core checkpoint kinase, ATR, and the 9-1-1 clamp in regulating recombination protein association at collapsed forks (Figure 5C). We closely correlate this regulation with the restraint recombination and speculate that that it provides one of several roles by which ATR maintains genome stability.

Materials & methods

Yeast strains and molecular biology

The *RuraR* (Lambert et al., 2005) plus the *uraR* and *Rura* loci (Lambert et al., 2010) used in this study have been previously described and the analysis of recombination outcomes was performed as previously described. Checkpoint deletions and alleles for the tagged proteins used were created and introduced via standard molecular and genetic techniques (Bahler et al., 1998; Moreno et al., 1991; Watson et al., 2008). Strains used are listed in supplementary Table 2. The *ade6-M375 int::pUC8/his3⁺/RTS1(A2)/ade6-L469* locus was a gift from Matthew Whitby (Ahn et al., 2005). All strains were grown in 30μM thiamine where indicated. The origins nearby *RTS1* were renamed as *ori3006/7*. We have previously used: *ars3003/4* (Miyabe et al., 2011) and *ars3004/5* (Lambert and Carr, 2005; Lambert et al., 2010; Mizuno et al., 2009; Mizuno et al., 2013).

2-dimensional gel electrophoresis

Replication intermediates (RIs) were analyzed and quantified by 2DGE as previously reported (Lambert et al., 2010). Briefly: Zymolyase-treated cells were embedded in an agarose plug, treated with proteinase K and washed several times in TE. After restriction digestion by *AseI*, RIs were enriched on BND cellulose columns, precipitated and separated by 2DGE using 0.35% and 0.9% agarose for the first and second dimensions, respectively. Quantification of RIs was performed using a phosphor-imager (Typhoon-trio) to detect ³²P-signal. Briefly, fork-termination and joint molecules signal were quantified as a % of stalled fork signal. Chromosomal rearrangements were analyzed by PFGE or Southern-blot as previously reported (Lambert et al., 2010; Lambert et al., 2005).

Visualisation of tagged proteins by ChIP

ChIP was carried out as previously described (Lambert et al., 2005), but with the use of a Diagenode Bioruptor at high setting (7 cycles: 30sec ON + 30sec OFF) for sonication to achieve a fragment size of 200-300 bp. Primers used for quantitative PCR (qPCR) are shown in Figure 2A and Supplementary Table 1. Enrichment was normalised to an internal control (*ade6* locus). Anti-GFP (rabbit polyclonal, Invitrogen), anti-Rpa2/Ssb2 (rabbit polyclonal, gift from Dr. Hisao Masukata), or anti human Rad51 (H-92 rabbit polyclonal, Santa Cruz) was used at 1:300, 1:500, or 1:100, respectively. Immuno-complexes were precipitated with

Dynabeads Protein G (Invitrogen). For each ChIP experiment, wild type and mutated strains have been analysed in parallel. The data (excepted Figure 1D) present the relative enrichment of immune-precipitated proteins in a given mutant relative to the enrichment observed in the corresponding wild type control strain either when the *RTS1*-RFB is active (arrest “on”) or inactive (arrest “off”).

Direct repeat recombination assay

Red colonies (*ade*⁻ cells) were picked from agar plates containing low adenine and no histidine, and inoculated in 10ml of rich media overnight. Cells were washed and split into two cultures each of 10ml Edinburgh Minimal Media (EMM) containing excess adenine and histidine, with or without thiamine. After 48 hours logarithmic growth, cells from each culture were plated onto YE agar plates containing excess guanine. Cells were concurrently plated onto non-selective media to determine the number of viable cells. After 3 days growth, colonies from the plates lacking adenine were counted to calculate the frequency of *ade*⁺ recombinants. Each experiment represents a median of 11 individual plates and statistical significance was calculated by using the students t-test.

Replication slippage assay

Replication slippage were scored using the reporter allele *ura4-sd20* that contains a duplication of 20 nt flanked by 5 nt of micro-homology and described in Iraqui 2012. DNA synthesis associated with HR-dependent fork-restart is error-prone, liable to replication slippage leading to the restoration of a functional *ura4*⁺ gene and thus an induction of *ura*⁺ colonies. Several single 5-FOA^R colonies were grown independently on uracil-containing plates with or without thiamine for 2-3 days, and then inoculated in uracil-containing media with or without thiamine for 2 days at 30°C. Appropriate dilutions were plated on supplemented minimal media and on uracil-free plates. Colonies were counted after incubation at 30°C for 5-7 days and the frequency of *ura*⁺ colonies was determined. Statistical significance was detected using the nonparametric Mann-Whitney U test.

Acknowledgments

We thank J.M.Murray and E.Hoffmann for helpful suggestions and members of the Carr and Murray labs for discussion and encouragement. II was funded by the Fondation pour la Recherche Medicale (FRM). ET, IM and AMC were supported by the MRC (Grant G1100074). SAEL was supported by the Institut Curie, the CNRS, ANR grants ANR-Piribio09-44854 and ANRJJC10-1203 01, and la Ligue contre le cancer (comité Essonne).

Author Contributions

AMC and SAEL designed the study and drafted the manuscript, ET, IM, II and JZ performed experiments. All authors helped interpret data and refine the manuscript.

References

- Ahn, J. S., Osman, F. and Whitby, M. C.** (2005). Replication fork blockage by RTS1 at an ectopic site promotes recombination in fission yeast. *EMBO J* **24**, 2011-23.
- Alabert, C., Bianco, J. N. and Pasero, P.** (2009). Differential regulation of homologous recombination at DNA breaks and replication forks by the Mrc1 branch of the S-phase checkpoint. *EMBO J* **28**, 1131-41.
- Bahler, J., Wu, J. Q., Longtine, M. S., Shah, N. G., McKenzie, A., 3rd, Steever, A. B., Wach, A., Philippsen, P. and Pringle, J. R.** (1998). Heterologous modules for efficient and versatile PCR-based gene targeting in *Schizosaccharomyces pombe*. *Yeast* **14**, 943-51.
- Bailis, J. M., Luche, D. D., Hunter, T. and Forsburg, S. L.** (2008). Minichromosome maintenance proteins interact with checkpoint and recombination proteins to promote s-phase genome stability. *Molecular and cellular biology* **28**, 1724-38.
- Barlow, J. H. and Rothstein, R.** (2009). Rad52 recruitment is DNA replication independent and regulated by Cdc28 and the Mec1 kinase. *EMBO J* **28**, 1121-30.
- Bastia, D., Zzaman, S., Krings, G., Saxena, M., Peng, X. and Greenberg, M. M.** (2008). Replication termination mechanism as revealed by Tus-mediated polar arrest of a sliding helicase. *Proc Natl Acad Sci U S A* **105**, 12831-6.
- Bester, A. C., Roniger, M., Oren, Y. S., Im, M. M., Sarni, D., Chaoat, M., Bensimon, A., Zamir, G., Shewach, D. S. and Kerem, B.** (2011). Nucleotide deficiency promotes genomic instability in early stages of cancer development. *Cell* **145**, 435-46.
- Biswas, S. and Bastia, D.** (2008). Mechanistic insights into replication termination as revealed by investigations of the Reb1-Ter3 complex of *Schizosaccharomyces pombe*. *Mol Cell Biol* **28**, 6844-57.
- Boddy, M. N., Lopez-Girona, A., Shanahan, P., Interthal, H., Heyer, W. D. and Russell, P.** (2000). Damage tolerance protein Mus81 associates with the FHA1 domain of checkpoint kinase Cds1. *Mol Cell Biol* **20**, 8758-66.
- Bolderson, E., Tomimatsu, N., Richard, D. J., Boucher, D., Kumar, R., Pandita, T. K., Burma, S. and Khanna, K. K.** (2010). Phosphorylation of Exo1 modulates homologous recombination repair of DNA double-strand breaks. *Nucleic acids research* **38**, 1821-31.
- Brown, E. J. and Baltimore, D.** (2003). Essential and dispensable roles of ATR in cell cycle arrest and genome maintenance. *Genes Dev* **17**, 615-28.
- Carr, A. M.** (2002). Checking that replication breakdown is not terminal. *Science* **297**, 557-8.
- Carr, A. M. and Lambert, S.** (2013). Replication Stress-Induced Genome Instability: The Dark Side of Replication Maintenance by Homologous Recombination. *Journal of molecular biology* **425**, 4733-4744.
- Casper, A. M., Nghiem, P., Arlt, M. F. and Glover, T. W.** (2002). ATR regulates fragile site stability. *Cell* **111**, 779-89.
- Cha, R. S. and Kleckner, N.** (2002). ATR homolog Mec1 promotes fork progression, thus averting breaks in replication slow zones. *Science* **297**, 602-6.
- Chen, S. H., Albuquerque, C. P., Liang, J., Suhandynata, R. T. and Zhou, H.** (2010). A proteome-wide analysis of kinase-substrate network in the DNA damage response. *The Journal of biological chemistry* **285**, 12803-12.

Cobb, J. A., Bjergbaek, L., Shimada, K., Frei, C. and Gasser, S. M. (2003). DNA polymerase stabilization at stalled replication forks requires Mec1 and the RecQ helicase Sgs1. *EMBO J* **22**, 4325-36.

Cobb, J. A., Schleker, T., Rojas, V., Bjergbaek, L., Tercero, J. A. and Gasser, S. M. (2005). Replisome instability, fork collapse, and gross chromosomal rearrangements arise synergistically from Mec1 kinase and RecQ helicase mutations. *Genes Dev* **19**, 3055-69.

Codlin, S. and Dalgaard, J. Z. (2003). Complex mechanism of site-specific DNA replication termination in fission yeast. *EMBO J* **22**, 3431-40.

Cotta-Ramusino, C., Fachinetti, D., Lucca, C., Doksani, Y., Lopes, M., Sogo, J. and Foiani, M. (2005). Exo1 processes stalled replication forks and counteracts fork reversal in checkpoint-defective cells. *Mol Cell* **17**, 153-9.

Dalgaard, J. Z. and Klar, A. J. (2001). A DNA replication-arrest site RTS1 regulates imprinting by determining the direction of replication at mat1 in *S. pombe*. *Genes Dev* **15**, 2060-8.

De Piccoli, G., Katou, Y., Itoh, T., Nakato, R., Shirahige, K. and Labib, K. (2012). Replisome stability at defective DNA replication forks is independent of S phase checkpoint kinases. *Molecular cell* **45**, 696-704.

Durkin, S. G., Arlt, M. F., Howlett, N. G. and Glover, T. W. (2006). Depletion of CHK1, but not CHK2, induces chromosomal instability and breaks at common fragile sites. *Oncogene* **25**, 4381-8.

El-Shemerly, M., Hess, D., Pyakurel, A. K., Moselhy, S. and Ferrari, S. (2008). ATR-dependent pathways control hEXO1 stability in response to stalled forks. *Nucleic Acids Res* **36**, 511-9.

Errico, A. and Costanzo, V. (2012). Mechanisms of replication fork protection: a safeguard for genome stability. *Critical reviews in biochemistry and molecular biology* **47**, 222-35.

Eydmann, T., Sommariva, E., Inagawa, T., Mian, S., Klar, A. J. and Dalgaard, J. Z. (2008). Rtf1-mediated eukaryotic site-specific replication termination. *Genetics* **180**, 27-39.

Froget, B., Blaisonneau, J., Lambert, S. and Baldacci, G. (2008). Cleavage of stalled forks by fission yeast Mus81/Eme1 in absence of DNA replication checkpoint. *Mol Biol Cell* **19**, 445-56.

Haghnazari, E. and Heyer, W. D. (2004). The DNA damage checkpoint pathways exert multiple controls on the efficiency and outcome of the repair of a double-stranded DNA gap. *Nucleic Acids Res* **32**, 4257-68.

Halazonetis, T. D., Gorgoulis, V. G. and Bartek, J. (2008). An oncogene-induced DNA damage model for cancer development. *Science* **319**, 1352-5.

Hartsuiker, E., Neale, M. J. and Carr, A. M. (2009). Distinct requirements for the Rad32(Mre11) nuclease and Ctp1(CtIP) in the removal of covalently bound topoisomerase I and II from DNA. *Mol Cell* **33**, 117-23.

Heichinger, C., Penkett, C. J., Bahler, J. and Nurse, P. (2006). Genome-wide characterization of fission yeast DNA replication origins. *EMBO J* **25**, 5171-9.

Hu, J., Sun, L., Shen, F., Chen, Y., Hua, Y., Liu, Y., Zhang, M., Hu, Y., Wang, Q., Xu, W. et al. (2012). The intra-S phase checkpoint targets Dna2 to prevent stalled replication forks from reversing. *Cell* **149**, 1221-32.

- Iraqui, I., Chekkal, Y., Jmari, N., Pietrobon, V., Freon, K., Costes, A. and Lambert, S. A.** (2012). Recovery of arrested replication forks by homologous recombination is error-prone. *PLoS genetics* **8**, e1002976.
- Jia, X., Weinert, T. and Lydall, D.** (2004). Mec1 and Rad53 inhibit formation of single-stranded DNA at telomeres of *Saccharomyces cerevisiae* cdc13-1 mutants. *Genetics* **166**, 753-64.
- Kai, M., Boddy, M. N., Russell, P. and Wang, T. S.** (2005). Replication checkpoint kinase Cds1 regulates Mus81 to preserve genome integrity during replication stress. *Genes Dev* **19**, 919-32.
- Kaochar, S., Shanks, L. and Weinert, T.** (2010). Checkpoint genes and Exo1 regulate nearby inverted repeat fusions that form dicentric chromosomes in *Saccharomyces cerevisiae*. *Proceedings of the National Academy of Sciences of the United States of America* **107**, 21605-10.
- Katou, Y., Kanoh, Y., Bando, M., Noguchi, H., Tanaka, H., Ashikari, T., Sugimoto, K. and Shirahige, K.** (2003). S-phase checkpoint proteins Tof1 and Mrc1 form a stable replication-pausing complex. *Nature* **424**, 1078-83.
- Kolodner, R. D., Putnam, C. D. and Myung, K.** (2002). Maintenance of genome stability in *Saccharomyces cerevisiae*. *Science* **297**, 552-7.
- Koundrioukoff, S., Carignon, S., Techer, H., Letessier, A., Brison, O. and Debatisse, M.** (2013). Stepwise activation of the ATR signaling pathway upon increasing replication stress impacts fragile site integrity. *PLoS genetics* **9**, e1003643.
- Krejci, L., Altmannova, V., Spirek, M. and Zhao, X.** (2012). Homologous recombination and its regulation. *Nucleic acids research* **40**, 5795-818.
- Lambert, S. and Carr, A. M.** (2005). Checkpoint responses to replication fork barriers. *Biochimie* **87**, 591-602.
- Lambert, S. and Carr, A. M.** (2013a). Impediments to replication fork movement: stabilisation, reactivation and genome instability. *Chromosoma* **122**, 33-45.
- Lambert, S. and Carr, A. M.** (2013b). Replication stress and genome rearrangements: lessons from yeast models. *Current opinion in genetics & development* **23**, 132-9.
- Lambert, S., Mason, S. J., Barber, L. J., Hartley, J. A., Pearce, J. A., Carr, A. M. and McHugh, P. J.** (2003). Schizosaccharomyces pombe checkpoint response to DNA interstrand cross-links. *Mol Cell Biol* **23**, 4728-37.
- Lambert, S., Mizuno, K., Blaisonneau, J., Martineau, S., Chanet, R., Murray, J. M., Carr, A. M. and Baldacci, G.** (2010). Homologous recombination restarts stalled replication forks at the expense of genome rearrangements by template exchange. *Molec. Cell* **39**, 346-359.
- Lambert, S., Watson, A., Sheedy, D. M., Martin, B. and Carr, A. M.** (2005). Gross chromosomal rearrangements and elevated recombination at an inducible site-specific replication fork barrier. *Cell* **121**, 689-702.
- Lee, B. S., Grewal, S. I. and Klar, A. J.** (2004). Biochemical interactions between proteins and mat1 cis-acting sequences required for imprinting in fission yeast. *Mol Cell Biol* **24**, 9813-22.
- Lindsay, H. D., Griffiths, D. J., Edwards, R. J., Christensen, P. U., Murray, J. M., Osman, F., Walworth, N. and Carr, A. M.** (1998). S-phase-specific activation of Cds1 kinase defines a subpathway of the checkpoint response in *Schizosaccharomyces pombe*. *Genes Dev* **12**, 382-95.

Lisby, M., Barlow, J. H., Burgess, R. C. and Rothstein, R. (2004). Choreography of the DNA damage response: spatiotemporal relationships among checkpoint and repair proteins. *Cell* **118**, 699-713.

Lopes, M., Cotta-Ramusino, C., Pelliccioli, A., Liberi, G., Plevani, P., Muzi-Falconi, M., Newlon, C. S. and Foiani, M. (2001). The DNA replication checkpoint response stabilizes stalled replication forks. *Nature* **412**, 557-61.

Lucca, C., Vanoli, F., Cotta-Ramusino, C., Pelliccioli, A., Liberi, G., Haber, J. and Foiani, M. (2004). Checkpoint-mediated control of replisome-fork association and signalling in response to replication pausing. *Oncogene* **23**, 1206-13.

Maudrell, K. (1993). Thiamine-repressible expression vectors pREP and pRIP for fission yeast. *Gene* **123**, 127-30.

Meister, P., Taddei, A., Vernis, L., Poidevin, M., Gasser, S. M. and Baldacci, G. (2005). Temporal separation of replication and recombination requires the intra-S checkpoint. *J Cell Biol* **168**, 537-44.

Mimitou, E. P. and Symington, L. S. (2008). Sae2, Exo1 and Sgs1 collaborate in DNA double-strand break processing. *Nature* **455**, 770-4.

Miyabe, I., Kunkel, T. A. and Carr, A. M. (2011). The major roles of DNA polymerases epsilon and delta at the eukaryotic replication fork are evolutionarily conserved. *PLoS genetics* **7**, e1002407.

Miyabe, I., Morishita, T., Shinagawa, H. and Carr, A. M. (2009). Schizosaccharomyces pombe Cds1Chk2 regulates homologous recombination at stalled replication forks through the phosphorylation of recombination protein Rad60. *Journal of cell science* **122**, 3638-43.

Mizuno, K., Lambert, S., Baldacci, G., Murray, J. M. and Carr, A. M. (2009). Nearby inverted repeats fuse to generate acentric and dicentric palindromic chromosomes by a replication template exchange mechanism. *Genes Dev* **23**, 2876-86.

Mizuno, K., Miyabe, I., Schalbetter, S. A., Carr, A. M. and Murray, J. M. (2013). Recombination-restarted replication makes inverted chromosome fusions at inverted repeats. *Nature* **493**, 246-9.

Moreau, S., Ferguson, J. R. and Symington, L. S. (1999). The nuclease activity of Mre11 is required for meiosis but not for mating type switching, end joining, or telomere maintenance. *Mol Cell Biol* **19**, 556-66.

Moreau, S., Morgan, E. A. and Symington, L. S. (2001). Overlapping functions of the Saccharomyces cerevisiae Mre11, Exo1 and Rad27 nucleases in DNA metabolism. *Genetics* **159**, 1423-33.

Moreno, S., Klar, A. and Nurse, P. (1991). Molecular genetic analysis of fission yeast Schizosaccharomyces pombe. *Methods in enzymology* **194**, 795-823.

Morin, I., Ngo, H. P., Greenall, A., Zubko, M. K., Morrice, N. and Lydall, D. (2008). Checkpoint-dependent phosphorylation of Exo1 modulates the DNA damage response. *EMBO J* **27**, 2400-10.

Myung, K., Datta, A. and Kolodner, R. D. (2001). Suppression of spontaneous chromosomal rearrangements by S phase checkpoint functions in Saccharomyces cerevisiae. *Cell* **104**, 397-408.

Myung, K. and Kolodner, R. D. (2002). Suppression of genome instability by redundant S-phase checkpoint pathways in Saccharomyces cerevisiae. *Proc Natl Acad Sci U S A* **99**, 4500-7.

Pandita, R. K., Sharma, G. G., Laszlo, A., Hopkins, K. M., Davey, S., Chakhparonian, M., Gupta, A., Wellinger, R. J., Zhang, J., Powell, S. N. et al. (2006). Mammalian Rad9 plays a role in telomere stability, S- and G2-phase-specific cell survival, and homologous recombinational repair. *Mol Cell Biol* **26**, 1850-64.

Raynard, S., Niu, H. and Sung, P. (2008). DNA double-strand break processing: the beginning of the end. *Genes Dev* **22**, 2903-7.

Sabatinos, S. A., Green, M. D. and Forsburg, S. L. (2012). Continued DNA synthesis in replication checkpoint mutants leads to fork collapse. *Molecular and cellular biology* **32**, 4986-97.

Segurado, M. and Diffley, J. F. (2008). Separate roles for the DNA damage checkpoint protein kinases in stabilizing DNA replication forks. *Genes Dev* **22**, 1816-27.

Segurado, M. and Tercero, J. A. (2009). The S-phase checkpoint: targeting the replication fork. *Biol Cell* **101**, 617-27.

Smolka, M. B., Albuquerque, C. P., Chen, S. H. and Zhou, H. (2007). Proteome-wide identification of in vivo targets of DNA damage checkpoint kinases. *Proceedings of the National Academy of Sciences of the United States of America* **104**, 10364-9.

Sogo, J. M., Lopes, M. and Foiani, M. (2002). Fork reversal and ssDNA accumulation at stalled replication forks owing to checkpoint defects. *Science* **297**, 599-602.

Sorensen, C. S., Hansen, L. T., Dziegielewska, J., Syljuasen, R. G., Lundin, C., Bartek, J. and Helleday, T. (2005). The cell-cycle checkpoint kinase Chk1 is required for mammalian homologous recombination repair. *Nat Cell Biol* **7**, 195-201.

Stracker, T. H., Usui, T. and Petrini, J. H. (2009). Taking the time to make important decisions: the checkpoint effector kinases Chk1 and Chk2 and the DNA damage response. *DNA repair* **8**, 1047-54.

Sun, W., Nandi, S., Osman, F., Ahn, J. S., Jakovleska, J., Lorenz, A. and Whitby, M. C. (2008). The FANCM ortholog Fml1 promotes recombination at stalled replication forks and limits crossing over during DNA double-strand break repair. *Mol Cell* **32**, 118-28.

Symington, L. S. (2002). Role of RAD52 epistasis group genes in homologous recombination and double-strand break repair. *Microbiol Mol Biol Rev* **66**, 630-70.

Tercero, J. A. and Diffley, J. F. (2001). Regulation of DNA replication fork progression through damaged DNA by the Mec1/Rad53 checkpoint. *Nature* **412**, 553-7.

Tsubouchi, H. and Ogawa, H. (2000). Exo1 roles for repair of DNA double-strand breaks and meiotic crossing over in *Saccharomyces cerevisiae*. *Mol Biol Cell* **11**, 2221-33.

Watson, A. T., Garcia, V., Bone, N., Carr, A. M. and Armstrong, J. (2008). Gene tagging and gene replacement using recombinase-mediated cassette exchange in *Schizosaccharomyces pombe*. *Gene* **407**, 63-74.

Zhu, Z., Chung, W. H., Shim, E. Y., Lee, S. E. and Ira, G. (2008). Sgs1 helicase and two nucleases Dna2 and Exo1 resect DNA double-strand break ends. *Cell* **134**, 981-94.

Zou, L. and Elledge, S. J. (2003). Sensing DNA damage through ATRIP recognition of RPA-ssDNA complexes. *Science* **300**, 1542-8.

Zubko, M. K., Guillard, S. and Lydall, D. (2004). Exo1 and Rad24 differentially regulate generation of ssDNA at telomeres of *Saccharomyces cerevisiae* cdc13-1 mutants. *Genetics* **168**, 103-15.

Figure Legends

Figure 1: The checkpoint proteins Rad3^{ATR} and Rad17 regulate recruitment of Rad52 at the *RuraR* locus.

A. Schematic representation of the *RuraR* locus. Grey and black lines indicate telomere and centromere proximal sides of the *ura4* gene, respectively. Blue boxes represent *RTS1*-RFB sequences and their polarity. The black arrow indicates the orientation of the *ura4* gene. The nearest replication origin (ori3006/7, grey circles) is located 5 kb *cen*-proximal to *RuraR*. *AseI* sites are ~1kb *cen* proximal and 0.6Kb *tel* proximal from *RTS1*.

B. Checkpoint pathways do not affect viability in the *RuraR* system. *RuraR* cells with the indicated genetic backgrounds were grown for 24 hours either with or without thiamine (replication arrest “off” and “on” respectively) and plated onto YE agar plates. The percentage of single cells (unable to divide), micro-colonies of <10 cells (unable to sustain division) and colonies with >10 cells were estimated after 18 hours. The *wt.* control strain contains the native *ura4* locus with no flanking *RTS1* sequences.

C. Analysis of replication intermediates (RIs) by 2-dimensional gel electrophoresis (2DGE) of DNA from indicated strains grown for 24 hours in media containing or lacking thiamine (fork-arrest “off” and “on” respectively). Top panels are diagrams of RIs within the *AseI* restriction fragment analyzed by 2DGE in indicated conditions. Numbers indicate the percentage of forks arrested by the *RTS1*-RFB \pm standard deviation (SD).

D. Regulation of Rad52 recruitment to *RuraR*. Chromatin immunoprecipitation (ChIP) of Rad52-GFP followed by quantitative PCR (qPCR) was carried out on the indicated *RuraR rad52-GFP* strains after 40 hours growth either with or without thiamine (arrest “off” and “on” respectively). Cells containing the *RuraR* locus in a checkpoint proficient (*wt*) background were analysed alongside an isogenic strain harboring the *rad3-d* alleles. Grey and black lines indicate telomere and centromere proximal side of the *ura4* gene, respectively. The blue box represents the single *RTS1*-RFB and its polarity. Top panel: Mean enrichments from three independent experiments are plotted, with error bars denoting \pm standard error of the mean (SEM). Bottom panel: Mean enrichments in *rad3-d* strain relative to the *wt* strain. Values are the mean from three independent experiments, with errors bars denoting \pm 95% confidence interval (CI). Thus, when the errors bars do not overlap the red dotted line (relative enrichment of 1), the level of Rad52 enrichment observed in *rad3-d*

strain is significantly different from the ones observed in the *wt* strain with $p < 0.05$. Numbers indicate the distance from the *RTS1*-RFB in KB on the telomere (-) and centromere-proximal (+) sides, the closest RFB to *ori3006/7* being used as referential (0).

E. Rad52-GFP enrichment relative to *wt* in *rad17-d* strain, as described on D. Values are the mean from two to three independent experiments, with $\pm 95\%$ CI.

F. Rad52-GFP enrichment relative to *wt* in the double mutant *rad3-d rad17-d* as described on D. Values are the mean from two to three independent experiments, with $\pm 95\%$ CI.

Figure 2: Rad3^{ATR} and Rad17 regulate Exo1-dependent recruitment of single stranded DNA binding proteins at collapsed forks.

A. Rad52-GFP enrichment relative to *wt* at the *RuraR* locus in the indicated strains, as described on Figure 1D. Values are the mean from three independent experiments, with $\pm 95\%$ CI. Grey and black lines indicate telomere and centromere proximal side of the *ura4* gene, respectively. Blue boxes represent the *RTS1*-RFBs and their polarity.

B. Schematic representation of the *uraR* locus. Grey and black lines indicate telomere and centromere proximal side of the *ura4* gene, respectively. The blue box represents the single *RTS1*-RFB and its polarity. The black arrow indicates the orientation of the *ura4* gene.

C. Relative enrichment of Rad52-GFP (top panel), Rad51 (middle panel) and RPA (bottom panel) relative to *wt* in indicated strains, as described for Figure 1D. ChIP followed by qPCR was carried out on the indicated *uraR* strains after 40 hours growth either with or without thiamine (arrest “off” and “on” respectively). Values are the mean from three independent experiments, with $\pm 95\%$ CI.

Figure 3: Exo1-dependent fork-resection is regulated by Rad3^{ATR} and Rad17.

A. Schematic representation of the *uraR* locus as presented on Figure 2B. Panels are diagrams of RIs within the *Ase1* restriction fragment analyzed by 2DGE in indicated conditions.

B. Analysis of RIs by 2DGE from indicated strains after growth for 24 hours in media with or without thiamine (fork-arrest “off” and “on” respectively). Numbers indicate the percentage of forks arrested by the *RTS1*-RFB \pm SD.

C. Quantification of termination signal from panel B in indicated strains. Values are the mean of three independent experiments \pm SD.

Figure 4: Increased replication slippage correlates to increased RPA recruitment.

A. Assays of fork-arrest-induced replication slippage. The *ura4-sd20* allele contains a duplication of 20 bp flanked by 5 bp of micro-homology and is non-functional: cells are thus auxotroph for uracil. Upon activation of the *RTS1*-RFB, the recombination-dependent restart of DNA synthesis is error-prone and liable to replication slippage, leading to the deletion of the duplication and thus the restoration of a functional *ura4* gene: cells are thus prototroph for uracil. Grey and black lines indicate telomere and centromere proximal side of the *ura4* gene, respectively. The blue box represents the single *RTS1*-RFB and its polarity. The *ura4-sd20* allele is either located downstream (construct 2) or upstream (construct 3) of the *RTS1*-RFB. Construct 1 is the control without any *RTS1*-RFB that is used to score the spontaneous frequency of replication slippage for each genetic background when Rtf1 is expressed. Serial dilutions of cells from indicated strains were spotted onto media containing or lacking uracil after growth in media without thiamine (Rtf1 being always expressed).

B. Frequency of *ura*⁺ reversion in the indicated strains and constructs, when Rtf1 is expressed (+, in media containing no thiamine) or not (-, in media containing thiamine). Values are the mean of at least three independent experiments \pm 95 % CI. Statistical significance was detected using the nonparametric Mann-Whitney U test. * indicates significant difference in the frequency of replication slippage upon activation of the *RTS1*-RFB (construct 2 or 3, Rtf1⁺) compared to the frequency observed in the strain containing no *RTS1*-RFB upon Rtf1 expression (construct 1, *rtf1*⁺).

Figure 5: Rad3^{ATR} regulates *ade6* recombination in an Exo1-dependent manner.

A. Schematic representation of the *ade6* recombination system. Recombination between the *ade6* heteroalleles can occur via conversion (bottom left) or deletion (bottom right) pathways. White and black circles represent the mutations in the *ade6* ORFs.

B. *ade6* recombination frequency was scored in indicated strains following 48 hours growth either with or without thiamine (fork-arrest “off” and “on” respectively). Cells were plated onto adenine-deficient media containing thiamine at baseline (T0). Mean frequencies from three independent experiments with error bars denoting \pm SD.

C. Simplified cartoon indicating that Rad3^{ATR}/Rad26^{ATRIP} (R3/R26) and the 9-1-1 complex regulate Exo1 to reveal ssDNA that associates with RPA and recombination proteins (Rad52 (52) is shown) when the replisome (Rep) is no longer competent.

Figure S1: Activation of the *RTS1*-RFB does induce cell cycle delay.

Strain containing the *RuraR* locus and harboring the *cdc25-22* allele were grown at 25 °C in minimal media with (arrest off) or without thiamine (arrest on) for 24 hours, then synchronized in G2 at 36°C for 4 hours and released at 25 °C. Samples was taken at the indicated times and analyzed for septation index (an S-phase marker) and DNA content by FACS.

Figure S2: The checkpoint kinases Cds1 and Chk1 and the nuclease activity of Mre11 are not required to regulate Rad52 recruitment to the *RuraR* locus.

A. Schematic representation of the *RuraR* locus. Grey and black lines indicate telomere and centromere proximal side of the *ura4* gene, respectively. Blue boxes represent the *RTS1*-RFBs and their polarity. *AseI* sites are ~1kb *cen* proximal and 0.6Kb *tel* proximal from *RTS1* (see Figure 1A for further details).

B. Rad52-GFP enrichment relative to *wt* at the *RuraR* locus in the *rad9-d* strains, as described for Figure 1D. ChIP of Rad52-GFP followed by qPCR was carried out on the indicated *RuraR rad52⁺-GFP* strains after 40 hours growth either with or without thiamine (arrest “off” and “on” respectively). Cells containing the *RuraR* locus in a wild type (*wt*) background were analysed alongside an isogenic strain harboring the *rad9-d* alleles. Values are the mean from two to three independent experiments, with \pm 95% CI. **C.** An equivalent experiment for the *chk1-d* (top panel) and *cds1-d* (bottom panel) strain.

Figure S3: Checkpoint pathways do not affect template exchange occurring during the restarting of the fork at *RuraR*.

A. Diagram of the *RuraR* locus (see Figure 1 for details). Upon fork-arrest at the *RTS1*-RFB stalled nascent strands switch template and invade the opposite *RTS1* sequence, leading to the formation of an early joint-molecule (D-loop). The incoming of the opposite fork leads to a reciprocal template switch of stalled nascent strands leading to the formation of a late joint-molecule containing Holliday junctions (HJs). The resolution of HJ-like structures leads to three distinct products: acentric or dicentric isochromosomes and the inversion of *ura4* orientation.

B. Analysis of RIs by 2DGE from indicated strains grown in media containing or lacking thiamine (fork-arrest “off” and “on” respectively). Top panels are diagrams of RIs within the

Ase1 restriction fragment analysed by 2DGE in indicated conditions. Numbers indicate the percentage of forks arrested by the *RTS1*-RFB \pm standard deviation (SD). The panels from *wt* and *rad3-d* strains are also presented on Figure 1C.

C. Quantification of joint-molecules observed in Panel B. Values are the mean of three independent experiments \pm SD.

D. Top panel: chromosomes from indicated strains and conditions were separated by Pulse Field Gel Electrophoresis (PFGE) and analysed by Southern-blotting using an *rng3* probe, located *telomere*-proximal from *ura4*. Cells were grown for 48 hours in media with (fork arrest “off”) or without thiamine (fork-arrest “on”). Bottom panel: Quantification of the acentric level in indicated strains and conditions. Values correspond to the mean of three independent experiments \pm SD.

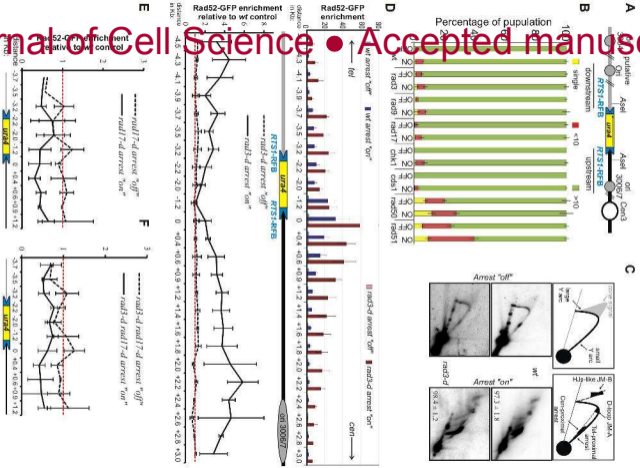
E. Top panel: representative Southern blot showing accumulation of rearrangement following digestion of genomic DNA with *EcoRV*, Southern blotting and hybridisation with a *ura4* probe. Cells from indicated strains were grown for 48 hours with (fork-arrest “off”) or without (fork-arrest “on”) thiamine. Bottom panel: quantification of the amount of chromosomal rearrangements observed in the top panel. Values correspond to the mean of three independent experiments \pm SD.

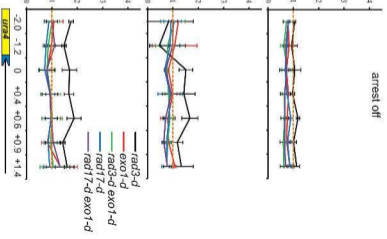
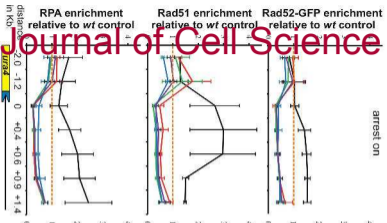
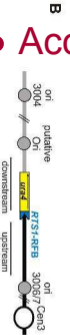
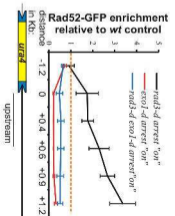
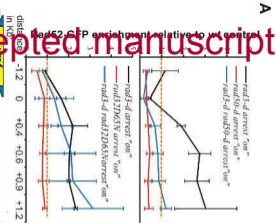
Table S1. qPCR primers used for ChIP

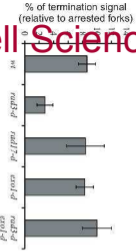
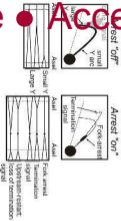
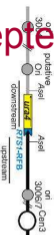
Primes used in ChIP analysis. Size = amplicon size in bp

Table S2. Strains used.

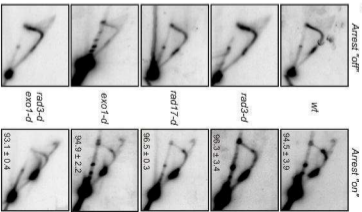
Strains used in this study.

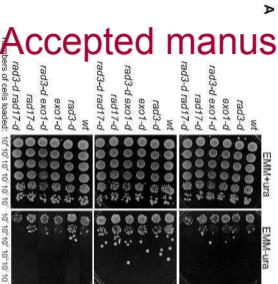




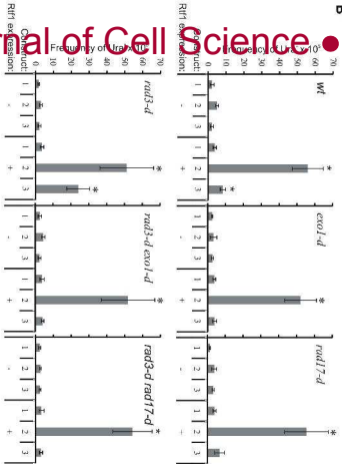


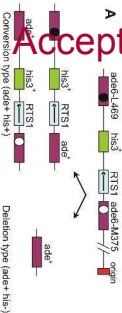
B



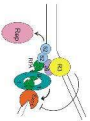


B





C



Frequency of Ade⁺ X 10⁻⁴

